

Review of Geant4 Applications in Radiobiology

Sara Mohammadi¹, Mahdy Ebrahimi Loushab², Mohammad Taghi Bahreyni Toossi^{*1}

1. Medical Physics Research Center, Mashhad University of Medical Sciences, Mashhad, Iran

2. Department of Physics, Faculty of Rajaei, Quchan Branch, Technical and Vocational University (TVU), Khorasan Razavi, Iran.

ARTICLE INFO

Article type:
Review Article

Article history:

Received: May 21, 2018

Accepted: Aug 04, 2018

Keywords:

Monte Carlo Method
Radiobiology
Cell Survival
Relative Biological
Effectiveness
Single Strand Break
Double-Strand Break
Particle Therapy

ABSTRACT

Introduction: Ionizing radiation is widely used in industry and medicine; however, it causes a significant health hazard by making microscopic damage to living tissue. Various biological parameters, including cell survival fraction and relative biological effectiveness, are taken into account to assess the severity and extent of biological damages. Microdosimetry suffers from various shortcomings and limitations, but the development of some powerful simulation software has paved the way to resolve these problems in recent years.

Material and Methods: In this study, the authors were looked for two keywords (Geant4 and radiobiology) in the title, abstracts, and keywords of Scopus and PubMed database articles.

Results: More than 100 articles were found. The researchers extracted the articles that were devoted to the construction of different geometries for DNA, nucleus, and cells as simulate the parameters, such as relative biological effectiveness, SF, linear energy transfer, and single-strand breaks/double-strand breaks in the present study.

Conclusion: Geant4 is one of the software commonly used to simulate biological factors. It has many properties, such as the ability to follow up physical processes in very low energy, open source code, and flexibility in complex geometries. In this paper, we reviewed some of the radiobiological parameters simulated with Geant4.

► Please cite this article as:

Mohammadi S, Ebrahimi Loushab M, Bahreyni Toossi MT. Review of Geant4 Applications in Radiobiology. Iran J Med Phys 2019; 16: 255-263. 10.22038/ijmp.2018.31823.1375.

Introduction

Parameters, such as kinetic energy released per unit mass, absorbed dose, energy fluence, linear energy transfer, and stopping power are calculated by macroscopic dosimetry. However, a systematic study and the quantification of the spatial and temporal distribution of absorbed energy attributed to random deposition of energy require the implementation of micro-dosimetry [1].

The size of a critical biological target (a cell or DNA molecule) defines the approach for the selection of a suitable dosimetry method. Micro-dosimetry is used to quantify biological quantities, such as relative biological effectiveness (RBE) and cell survival fraction, while nano-dosimetry is employed to estimate single and double strand breaks (SSB and DSB) as well as the distribution of ionization cluster size [2].

A key point regarding the beam interaction with bio-structures is the level of absorbed dose in normal tissue. In real laboratory conditions, micro and/or nano dosimetric methods are unable to calculate the absorbed dose in a target with micro or nano dimensions. Under such circumstances, simulation is offered as a highly effective alternative method.

However, it is essential to investigate the estimated dose verified by laboratory measurement.

Given the random nature of dose distribution in a target, simulating methods based on track structures are used extensively. In fact, track structure studies allow researchers to compute dosimetric quantities related to the biological effects of ionizing radiation in various fields. Moreover, track structure studies are particularly useful in the case of several consecutive events when direct measurement is not possible [3].

There are various methods to describe a track, which may range from a simple track with one parameter to complicated 4D Monte Carlo approach known as track-structure codes. Methods based on track-structure are sometimes based on the analytical solutions, which solve the transport equation of particles in the material [4]. Another technique is to find a numerical model based on sampling of the interaction of the particles with the nucleus [5].

The common approaches of track-structure codes are as follows: track methods related to the target, which are based on a track with one parameter [6], track methods founded upon mean radial dose curve due to the trajectories of charged particle without considering the stochastic structures of the tracks [7],

*Corresponding Author: Tel: +98 51 38828576; Fax: +98 51 38002320; Email: bahreynimt@mums.ac.ir

condensed-history Monte Carlo (CHMC) method, which provides an average over discrete particle histories. The CHMC method includes a large number of codes with different goals among which FLUKA, MCNP5, MCNPX, PENELOPE, and Geant4 are the most widely used [8-12]. On the other hand, the full 3D Monte Carlo track-structure codes simulate detailed information on all elastic and inelastic interactions during the transport of each particle to the target. In addition, one could consider 4D codes which introduce the time parameter in the 3D Monte Carlo track-structure method [13].

PARTRAC is one of the 4D codes that consists of different modules with defined data interfaces. These interfaces describe the stages of radiation interaction and radiation response [14, 15]. The code covers a large number of concepts concerning the biologic effect of beams on various physical, physicochemical, and biologic levels [16]; however, it cannot be used widely due to its unavailability to all researchers.

In most Physics-List packages Monte Carlo codes (e.g. electromagnetic standard packages) are used although the applicability is limited to the lower threshold of 1 keV. However, for microdosimetry applications, Geant4 Low Energy Electromagnetic package presumes a minimum energy limit of secondary production of about 250 eV [17]. For radiobiological studies, especially microdosimetry applications, general purpose Monte Carlo codes do not provide enough physical functionality to date. For this specific situation, "track structure code" is considered as a specialized version of Monte Carlo [18].

Most of Monte Carlo codes for track structure method have neither been open source, nor are their software libraries available for public use. However, the Geant4 toolkit, which has been used in the current study to examine microdosimetry, is open source. In this regard, the investigations based on this code could be considered as a methodological innovation in the field. As a computational method, track structure simulation provides an important tool for biological research [18] supplying guidelines to the experimental activity. When the evaluation of the findings is only possible based on theoretical analysis, the present approach provides a "new paradigm" in biological research [19].

Geant4 is a software toolkit used to simulate the passage of particles through matter [20, 21], which can process the measurement of bio-molecules in the low energies. The main aim of this software is to develop models that describe biologic systems, including cells and DNA, as well as models that explores biologic procedures. With these abilities, Geant4 excels all other types of available codes [22]. For the first time, Geant4-DNA [23], one of the general-purpose Monte Carlo system, can simulate biological effects of radiation with biological systems at the cellular and molecular DNA level [24]. Geant4-

DNA provides a wide range of new applications ranging from oncological radiotherapy to protection of astronauts from radiation due to its potentiality to simulate biological effects of radiation and to function at an advanced level in other simulation domains, such as geometry, physics, and interaction tools [22].

Geant4 Simulation Toolkit

The toolkit is responsible for runs, events, and tracks. Geant4 can simulate static and kinematic quantities of the events, as well as primary and secondary particles. The tracking, which is calculated by the physical interactions, manages the transport of the track.

Geant4 toolkit allows the modeling of the experimental setups in details. Boundary-represented solids and the representations of shape geometry (e.g. constructive solid geometry) are supported by ISO STEP standard. Geometry and body parts of the patient, as well as external or internal radioactive sources and detectors could be defined in the similar framework, which support the strength and adaptability of the Geant4.

Geant4 Hadronic Physics offers parameterization-based models along with various therapy-driven models. In addition, the treatment of low-energy neutron transport falls in the domain of the toolkit. In the toolkit definitions of particles compliant to particle data group, hundreds of baryonic, mesonic resonances, and ions, as well as their decay processes and models have been considered [23].

Geant4 Electromagnetic Physics is responsible for the management of photon, muon, and lepton interactions, as well as the electromagnetic interactions of hadrons and ions. It provides multiple implementations of ionization, bremsstrahlung, multiple scattering, photoelectric effect, Compton effect (also with polarization) along with properties, such as handling annihilation, pair conversion, synchrotron and transition radiation, scintillation, refraction, reflection, absorption, Raleigh scattering, Auger electron, and fluorescence. In addition, the implementation of low energy processes down to 250 eV for photons, electrons, hadrons, and ions characterizes multiple models. Geant4 Electromagnetic Physics is appropriate for accurate physics in the biomedical domain due to its low energy extensions.

Geant4 medical physics applications

Researchers can benefit from advanced Geant4 tools in the field of diagnostics medicine, and therapy. They are intended to assess the existing techniques and treatments planning system, where there is a need for accurate dose estimation.

Geant4 is a unique software for medical physics, which can define homogeneous or heterogeneous media of biological interest, flexible enough to model

complex geometry. Additionally, Geant4 is capable of fully simulating steering runs, events, and tracks in any geometry, as well as visualizing experimental set-up with a simple user interface. Considering all these properties, Geant4 Simulation Toolkit offers a powerful tool for medical physics. Geant4 applications in medical physics include:

a) Radiotherapy: External beam radiotherapy [25] and intensity-modulated radiation therapy [26], brachytherapy [25], hadrontherapy [27] proton and carbon ion therapy [28] and metabolic therapy of thyroid diseases [20].

b) Other dosimetric studies at cellular level [29], microdosimetry [30, 31], and nanodosimetry [32].

c) GATE: A new general purpose simulation platform for PET and SPECT applications. GATE is a Geant4 application for simulating tomographic emission [33]. Today, this code is also used in radiotherapy, brachytherapy, and patient dosimetry.

Geant4 new projects in bio-medicine

a) Geant-4 DNA: Considering that biological effects are studied in a top-down manner, a new bottom-up approach has been introduced by the European Space Agency, which analyses nano-scale effects of energetic particles at the DNA level.

b) Shielding in space missions [34].

A project was initiated at INFN, Genova, Italy in order to perform studies on radiation shielding in space missions using Geant4 Simulation Toolkit [35].

Materials and Methods

Geant4 in Radiobiology

In the studies on radiobiology simulation, geometry is of utmost importance. In microdosimetric studies, the areas of investigation are the shape of cell, nucleus, and their dimensions [36], as well as the position of a single cell, monolayer cell, or cell cluster [37]. On the other hand, the effects of the polystyrene material on the flask bottom have been explored in many studies, which contribute to the accuracy of the results. In nanoscale studies, the DNA sequence has been simulated using various methods with different levels of accuracy and precision. Furthermore, there has been the simulation of different breaks caused by the beam collisions.

In 2013, Raisali et al. [32] examined the number of SSB and DSB of DNA caused by direct and indirect damages to Auger electrons resulted from the decay of ^{123}I and ^{125}I isotopes by simulation with the Geant4-DNA toolkit. They introduced a model designed by Bernal and Liendo model (2009) as the primary model, which included a similar geometric model containing more details about the DNA spiral as another model in the simulation (Figure 1). The utilization of a simple mechanism acts on the threshold of the particle energy. This means that if the energy transfer in direct collision with the phosphate-sugar group is greater than 10eV, SSB is implemented and the minimum energy of 17eV is required for an indirect collision to create a radical

pair. If a decay causes two breaks in DNA at a distance of less than 10 bp, it is important to consider DSB.

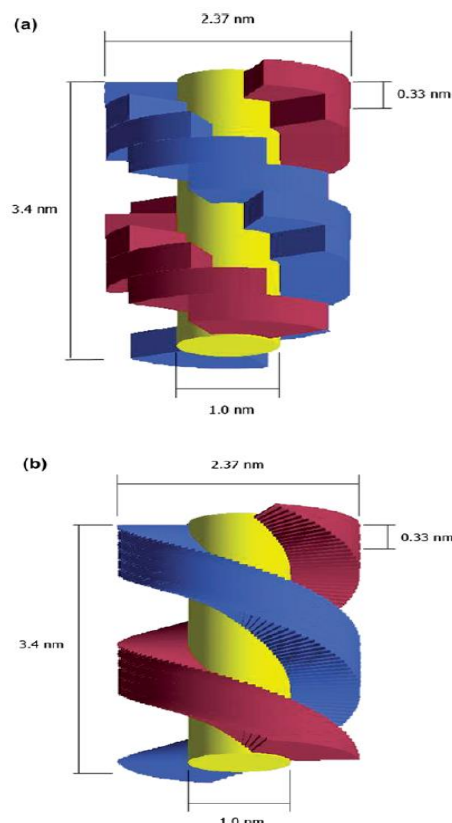


Figure 1. Geometric structures used to simulate the DNA strand

Figure (a) shows 41 base pairs and Figure (b) Shows more details about DNA [32].

The results showed that the use of the initial model is sufficient to predict direct damages. However, to elaborate on damages caused by the indirect collision of the beam, it is necessary to employ precise models in the DNA spiral. Finally, it was argued that the results of this method were consistent with the experimental results were obtained from the Comet assay and it was suited for nano-dosimetry calculations.

In many studies, the effects of gamma rays [38], an electron beam of various energies [39], mechanism of direct and indirect damage, and SSB and DSB with different geometries for the DNA strand have been discussed, which were in favour of a nano-dosimetry method.

The processes currently undertaken in Geant4 describe elastic and inelastic scattering interactions, such as excitation and ionization for electrons, protons, neutral hydrogen, an alpha particle, and helium. The range of energy is from 7.4 eV (the lowest energy level of excitation potential of the water) to 10 keV for electrons, and for proton and light ions ranges from 100 eV/u to 10 MeV/u [17, 40].

Geant4 can model radiation biology in four stages as follows:

- **Geometry stage:** It includes the simulation of DNA strands, chromatin fiber, chromosomes, whole-cell nucleus, and individual cells.
- **Physical stage:** Step-by-step modeling of the physical interactions between ionizing radiation and biological medium (water), including the excitation and ionization of water molecules and generation of solvated electrons.
- **Physico-chemical/chemical stage:** This stage consists of molecular species production, diffusion, and mutual interactions. Under ionizing radiation, excited and ionized water molecules may decay and dissociate into new molecules (e^-_{aq} , H_2 , H^{\bullet} , $^{\bullet}OH$, and H_3O^+), which can diffuse and interact mutually to produce other molecules (OH^{\bullet} , H_2O_2). These e^-_{aq} , H_2 , H^{\bullet} , $^{\bullet}OH$, and H_2O_2 species can also directly interact with DNA components [41].
- **Biological damages:** This stage covers direct DNA damages (physical damages) in the period of 0 to 10^{-15} seconds and indirect DNA damages (physiochemical damages) from 10^{-15} to 10^{-5} seconds [42].

The biological effects of radiation vary from cell killing to mutation in genome cells and even carcinogenesis [43].

Significant Factors in Radiobiology

Cell Survival Ratio

Cell survival fraction is one of the most frequently used aspects in radiobiology. In radiobiology studies, if the cell does not have the ability to measure proliferation, it is considered dead. This means that the cell is physically present in the biological system; however, it loses the capacity to multiply indefinitely or produce many progenies [44, 45].

On the other hand, the survival of curve depends on a variety of properties, such as a cell-line response, radiation quality, and dose rate [22]. Different methods can be divided into two groups with regard to cell survival.

- a) Target theory models
 - Single-hit model
 - Multi-target single-hit model
 - Single-target multi-hit model
- b) Molecular theory models
 - Theory of Radiation Action
 - Theory of Dual Radiation Action
 - Repair-Misrepair Model
 - Lethal-potentially Lethal Model [45]

i. Cell Survival Fraction in Targeted Alpha Therapy

In Targeted Alpha Therapy, vasculature system inevitably absorbs a background radiation dose through activity in the blood. In this regard, Huang et al. [46] randomly emitted alpha particles from within the

capillary lumen to investigate whether the lymphocyte and capillary endothelial cells would be damaged by the background dose. Moreover, they modeled the lymphocyte cell and its nucleus as two ellipsoids with different centers. In addition, they made a tube with an oval nucleus on the internal wall to simulate the normal tissue capillary EC geometry.

One of the basic parameters in microdosimetry is the energy deposition ε arising from a single traversal of the target volume. Therefore, Huang et al. recorded and processed the energy deposition of an alpha particle and its secondary particles in the LC and EC nucleus.

The results showed that the means of energy deposited for an alpha particle traversing the LC and EC geometry were 274 and 226 keV with a mean Linear Energy Transfer of 73 and 66 keV/ μm , respectively. Accordingly, the specific energy per traversal over the nucleus target volume was 50 cGy for the LC geometry and 40 cGy for the EC nucleus, and spatial distribution of the events was used for obtaining the weighted average specific energies. The results revealed that the mean of z per decay was 1.4 cGy for the lymphocyte and 1.1 cGy for capillary cells.

Moreover, the alpha-immunoconjugate administered in the melanoma clinical trial showed up to 25 mCi of ^{213}Bi . The number of ^{213}Bi atoms ($t_{1/2}=2736$ s) in the activity of 25 mCi was 3.65×10^{12} . The ^{213}Bi concentration (C_{Bi}) was unchanged in each vessel; therefore, the total number of decay for three vessels of arteriole, capillary, and venules (30, 8, and 20 μm , respectively) was different. If we assume that there are 5 L of blood in the body, then ^{213}Bi concentration will be 7.3×10^{-4} atom/ m^3 .

Since the vessel diameter determined the number of traversals, the number of traversals was 0.29 in arteriole, 0.05 in the capillary and 0.19 in the venule. Furthermore, the background dose for one central LC nucleus of these vessels was 15.1, 2.5, and 9.6 cGy, respectively.

In the clinical trial case, the number of ^{213}Bi atoms in one capillary lumen volume of 2.5×10^{-12} liter ($\pi r^2 \times L$) was 1.8. The authors calculated the background dose in the case of lymphocytes cells by multiplying the specific energy of single ^{213}Bi disintegration and the total number of ^{213}Bi atoms that decay in the lumen. Thus, the estimated background dose for one normal tissue capillary nucleus was 2 cGy. To estimate the cell survival fraction by a biological cell inactivation model, the specific energy values can be used. Moreover, to calculate the cell surviving fraction following alpha particle irradiation, $S = e^{-D/D_0}$ is used. Where, D_0 is the dose that yields a 37% surviving fraction.

As a result, when the activity of Bi is 25 mCi, a background dose of 2 cGy corresponds to about 99% survival rate for normal capillary ECs. Moreover, the dose range of 2.5-15.1 cGy indicates 89% ~ 98% survival rate for LCs. A small number of endothelial cells and LCs that are lost are not considerable results [30]. They used this microdosimetry method to calculate

the background dose and maximum therapeutic gain for the systemic targeted alpha therapy.

The application of this method helped to determine the therapeutic gain in the targeted treatment with alpha-emitting isotopes, as well as the dose received by healthy tissue (D_{tissue}) and tumor tissue (D_{tumor}). The maximum therapeutic gain can be obtained by the following formula.

$$\text{Therapeutic gain} = \frac{D_{\text{tumor}}}{D_{\text{tissue}}} \quad (1)$$

This method yields high therapeutic gain for the targeted alpha emitter radioisotope, meaning that the dose received by the tumor tissue is much greater than the dose received by normal tissue. It demonstrates the accuracy and efficiency of this method.

ii. Cell survival in radiotherapy with Beta particles

If low LET radiation is used in radiotherapy, the single-hit equation ($S = e^{-D/D_0}$) will not be valid anymore. In addition to significant mechanisms of cell death, which are independent of dose rate (e.g., chromosomal damage), the probability of damage proportional to dose squares should be considered, as well.

$$S = \exp[-\alpha D - \beta D^2] \quad (2)$$

For beta-emitting radionuclide therapy, the survived fraction and biological factors (e.g., RBE) are calculated by the linear-quadratic model [29]. The linear-quadratic (LQ) model is most extensively used for cell survival analysis and description of other radiobiological endpoints [47].

Freudenberg et al. developed a method based on Geant4 simulations for nuclear medicine in 2011 [48]. They divided the absorption dose of cells into two distinct sections, namely self-dose, and cross dose. Furthermore, they performed simulations of each section separately for four different isotopes (i.e., Re-188, I-131, Y-90, and Tc-99m). In the next step, the researchers incorporated the calculated dose in simulations on the linear quadratic equation using constants α and β extracted from previous laboratory studies and calculated the cell survival fraction. On the other hand, the absorption dose resulted from the treatment of PCR C13 cells with a solution containing each of the isotopes was measured both in the presence and absence of perchlorate in the laboratory. In each case, the cell survival ratio was calculated by colony assay and the values of simulation survival fraction was compared to those obtained in laboratory experiments.

They drew a comparison between values obtained in their study and those reported by Cai [49] asserting that the results of the Geant4 simulation were more consistent with those reported in the MIRD analytical method, compared to the MCNP simulation [50]. Freudenberg et al., simulated the absorption dose of two isotopes, Tc-99m and I-123, in a cell of 7 μm and nucleus of 4 μm using two single-cell and monolayer models through the utilization of the above-mentioned method. They compared results with that of laboratory experiments on a cells of the same isotopes in the

presence and absence of perchlorate. They calculated the relative biological effect using $RBE = \frac{D_0}{D_{37}}$ [51] (3)

Undoubtedly, understanding the relationship between the characteristics of a given radiation and its induced damage pose a significant challenge.

Relative Biological Effectiveness (RBE)

The general effects of radiation on organisms have been extensively studied. It has been shown that radiation can influence the function, reproductive characteristics, and life cycle of cells. Experiments have also shown that DNA is the primary target by which radiation exerts its effects [52]. On the other hand, ionization in the nucleus can directly or indirectly damage the genetic material of the cell. The association between energy absorption from radiation and biological effect is well-established. However, according to the studies, the effect of radiation can also vary according to the type of incident radiation. The RBE is a measure that qualifies the effectiveness of damage caused by various types of ionizing radiation. The RBE is defined as the ratio of the dose of reference radiation, such as Co-60 to the dose of test beam, that is necessary to achieve the similar biological endpoint (it is an iso-effective dose ratio)[53]. The biological effects of radiation are naturally associated with the ionization of cell nuclear material. The ionization of nuclear material is in turn derived from energy transfer from an incident particle to the medium [54]. In fact, the pattern of energy deposited to the medium at the microscopic level is the reason for this difference.

The RBE is different for each cell line. Generally, some mammalian cells are characterized by a survival curve with a broad shoulder, with split-dose experiments indicating a substantial amount of sublethal damage repair that has high RBE. Other cell types show a survival curve with a minimal shoulder, which is reflected in the more restricted repair of sublethal damage and thus have low RBE.

There is a variety of methods to measure RBE in Geant4. The RBE could be measured by cell survival models or by measuring SSB or DSB. In many studies, the Geant4 code has been used to calculate the relative biologic effect during the collision of heavy charged particles with the substance [55-57]. Also in these studies, the authors calculated the values of constant α and β , using the method of "Microdosimetric Kinetic Model" proposed by Kase et al. [58].

Burigo et al.[59] determined RBE based on the linear quadratic model in cell survival after radiation (Eq 2). On the other hand, following the application of a modified MK model to the tumor cells of the human salivary gland (HSG), a parameter α is estimated as:

$$\alpha = \alpha_0 + \frac{\beta}{\rho \pi r_d^2} y^* \quad (4)$$

Where, α_0 is a constant value equals to 0.13 (1/Gy) indicating the initial SF curve slope when the limit of LET moves to zero, $\beta=0.05$ (1/Gy²) refers to a constant value and LET independent, ρ as the density of tissue

and $r_d=0.42$ (μm) is the radius of a sub-cellular domain in the microdosimetric-kinetic (MK) method. The fact that α -parameter of the linear-quadratic model depends on y^* rather than \bar{Y}_d shows the reduction of the RBE, which is known as the saturation effect. It suggests that if local energy deposition increases extremely then there is no increase of biological effects induced by high-LET radiations [60]. As presented here, the same value of parameter $\beta=0.05(1/\text{Gy}^2)$ can be used to fit the data on S with Eq (3) for X-rays and ions. This approves the assumption of the MK model according to which β is independent of LET.

According to the LQ model, the RBE_{10} for 10% survival of HSG cells is calculated using the following relation.

$$\text{RBE}_{10} = \frac{D_{10,R}}{D_{10}} = \frac{2\beta D_{10,R}}{\sqrt{\alpha-4\beta \ln(0.1)}-\alpha} \quad (5)$$

Where, D_{10} is the 10% survival dose of ions and $D_{10,R} = 5.0$ Gy denotes the 10% survival dose of reference radiation (250 kVp X-rays) for HSG cells [61]. Ultimately, the biological dose (D_{bio}) is calculated through RBE_{10} and physical dose [59].

$$D_{\text{bio}} = \text{RBE}_{10} D_0 \quad (6)$$

In an article conducted by Hosseini et al., the relative biological effectiveness was measured using the Geant4 toolkit. For this purpose, they determined the number of lesions on DNA strand. In addition, the damages were made to 2 opposite DNA strands at a distance of less than 10 bp (about 35 nm), where DSBs must be identified. To this end, the researchers first assessed the extent of damages on DNA strands, and then an algorithm was designed to identify lesion types and its class. The same procedure was applied to gamma rays, which were produced from cobalt-60, as a reference for the measurement of RBE [62].

$$\text{DSB}_{\text{ion}}(\text{Gbp}^{-1}\text{Gy}^{-1}) \times D_{\text{ion}} = \text{DSB}_{\text{ion}}(\text{Gbp}^{-1}) \quad (7)$$

$$\text{DSB}_{\text{Co}}(\text{Gbp}^{-1}\text{Gy}^{-1}) \times D_{\text{Co}} = \text{DSB}_{\text{Co}}(\text{Gbp}^{-1}) \quad (8)$$

Where, DSB_{ion} refers to the number of DSBs caused by the collision of the proton beam with the DNA strand. The DSB_{Co} is the number of DSBs caused by the collision of ^{60}Co gamma ray with DNA strand and D_{ion} and D_{Co} are the absorption dose of proton and cobalt.

If the number of DSBs caused by a collision between beam and DNA is assumed as the ultimate biological effect, the same number of breaks are required to achieve a similar effect from both beams. Therefore, the following relation is obtained.

$$\frac{\text{DSB}_{\text{ion}}(\text{Gbp}^{-1}\text{Gy}^{-1}) \times D_{\text{ion}}}{\text{DSB}_{\text{Co}}(\text{Gbp}^{-1}\text{Gy}^{-1}) \times D_{\text{Co}}} = 1 \quad (9)$$

$$\text{RBE} = \frac{D_{\text{Co}}}{D_{\text{ion}}} = \frac{\text{DSB}_{\text{ion}}(\text{Gbp}^{-1}\text{Gy}^{-1})}{\text{DSB}_{\text{Co}}(\text{Gbp}^{-1}\text{Gy}^{-1})} \quad (10)$$

Finally, the relative biologic effect for each radiation beam could be calculated relative to the reference beam using Geant4 simulation.

Linear Energy Transfer

The average energy transfer, which is obtained from purely “electronic” interactions (ionization or excitation) per unit length traveled by charged primary particles, can be defined as linear energy transfer (LET). The LET is strictly defined as a spatial point and thus its application is restricted by definition. It is because, in a practical problem, irradiated targets are always finite in volume rather than a dimensionless point, and therefore it is not easy to meet the monoenergetic prerequisites of the primary particles. Hence, the restricted definition of LET offers two different practical LET concepts called track-averaged LET (LET_t) and dose-averaged LET (LET_d). Guan et al. studied track-averaged LET and dose-averaged LET in proton therapy, by applying Monte-Carlo techniques [63]. As such, the reliability of the calculated RBE can be significantly affected by the accuracy of the calculated LET and the calculation method.

The following equation measures the track-averaged LET.

$$\text{LET}_t = \sum_{i=1}^n \left(\frac{\epsilon_i}{l_i}\right) \omega_{i,t} = \frac{\sum_{i=1}^n \left(\frac{\epsilon_i}{l_i}\right) l_i}{\sum_{i=1}^n l_i} = \frac{\sum_{i=1}^n \epsilon_i}{\sum_{i=1}^n l_i} \quad (11)$$

And dose-averaged LET (LET_d) is calculated in the following equation.

$$\text{LET}_d = \sum_{i=1}^n \left(\frac{\epsilon_i}{l_i}\right) \omega_{i,d} = \frac{\sum_{i=1}^n \left(\frac{\epsilon_i}{l_i}\right) \epsilon_i}{\sum_{i=1}^n \epsilon_i} = \frac{\sum_{i=1}^n \frac{\epsilon_i^2}{l_i}}{\sum_{i=1}^n \epsilon_i} \quad (12)$$

Where, n is the total number of charged particles, ϵ_i is the energy of i^{th} charged particle, and l_i is the tracking step length by i^{th} charged particle.

The selection of a proper LET as an input parameter for RBE modeling or as an indicator to explain the results of the biological experiment can be demanding. It should be noted that the beam energy diminishes along the path, and while the particle fluence drops to zero, the averaged LET rises.

In the dose plateau region, LET_t shows minor dependence while LET_d depicts a strong dependence on the step limit. The results of proton biology experiments have shown that in the dose plateau region, LET plays a trivial role in the determination of the cell killing [64]. Thus, LET_t is recommended for the dose plateau region due to its continuous increase along the beam path and step-limit independence. In the vicinity of the Bragg peak, LET_d is loosely dependent on step limit. For this reason, it is recommended to use LET_d around the Bragg peak. A spatial transition point is required to switch between the use of LET_t and LET_d to quantify the LET [63].

Discussion

One of the notable properties of Geant4 is the ability to calculate radiobiological parameters, such as SF and RBE, which are applied in microdosimetry. Given that each cell line has its own biological properties, some constants are added to simulations. Moreover, each radiation (alpha, beta and gamma rays) has its own

specific features, and therefore various methods are applied in the simulation. Consequently, there is no common method to simulate all radiobiological parameters.

Alpha particles have low penetration depth and thus the construction of small geometries (such as a single cell) rather than large geometries in MC simulation would yield accurate results, which in turn increases the speed of simulations.

These simulations require extremely low energy physical models, the equivalent range of which is as large as cell dimensions, leading to the application of low energy models of Geant4, such as PENELOPE and LIVERMOR, and therefore precludes the use of CHMC codes. These models can simulate electromagnetic interaction for the electron, positron, and photon particles with an approximate energy range of 250 eV. This minimum energy belongs to a dimension as large as cellular dimensions.

Unlike alpha particles, in the biological studies of low LET radiation, the situation is different for low LET radiation. When the simulation values and experimental values are compared, since the absorption doses obtained from the simulation encountered particle escape from the boundary, and the experimental absorption dose represents the average of these values, since the absorption doses obtained from the simulation encountered particle escape from the boundary, and the experimental absorption dose represents the average of these values. Therefore, the comparison of these values would not be accurate, and thus this point should be considered in future studies.

Generally, the simulations of high LET radiation (alpha particles) are run for one cell and the results are extended to all cells. Simulations for a low LET radiation, such as beta and gamma rays should cover larger dimensions in geometry since the range of these particles is larger than that of alpha particles, and they affect adjacent cells as well. Therefore, various methods can be designed to simulate a large geometry. Firstly, when dimensions of geometry are big enough to yield accurate parameters methods, such as LET, S-value, and SF, can be used, which prolong the MC simulation time. Secondly, a combination of several physical models in different volumes can be used to simultaneously increase accuracy and efficiency. In large volumes, transporting particles with low energy models is extremely time-consuming, and thus it is recommended to apply standard models with higher speed and lower precision. On the other hand, low energy models are suitable for small sensitive volumes, such as cell and DNA that require great precision. The third method is implemented in large dimensions with standard models, determining the spectra of particle energy on the sensitive volume. By the application of low energy models to the sensitive volume, micro/nanodosimetry quantities can be measured. In addition to saving time, one notable advantage of this method is a direct measurement of quantities (such as dose) in the

intermediate step, leading to verification of MC simulation results.

In radionuclide therapy, two methods are used for defining radioisotope as the primary particle source in order to simulate radioisotope effects. In most Monte Carlo simulations, the radioisotope decay spectrum, which involves the probability of producing any decay product, has been used and in most cases the tracking of products with low probability or products that their energy is relatively low compared to the original products, are disregarded [65]. However, in other approaches, including Geant4 toolkit, the entire decay process is simulated for the isotope, by activating the physics of radioactive decay. Since this method entails all particles, it is more accurate in comparison with the first method; however, its implementation would be time-consuming.

Conclusion

Geant4-DNA is a powerful tool in radiobiological studies, which can follow up physical processes in very low energy and flexibility in complex geometries. Based on these properties, these tools become more appropriate for the estimation of RBE, cell survival fraction, SSB/DSB, and LET.

Acknowledgment

I would like to thank Professor Barry J Allen for his expert advice.

References

1. Rabus H. Fundamentals of Micro- and Nanodosimetry. 2011.
2. Guatelli S. Radiotherapy Based On α Emitting Radionuclides: Geant4 for Dosimetry and Micro-/Nano-Dosimetry. 2013.
3. Nikjoo H, Uehara S, Emfietzoglou D, Cucinotta FA. Track-structure codes in radiation research. Radiation Measurements. 2006; 41(9-10):1052-74.
4. Butts J, Katz R. Theory of RBE for heavy ion bombardment of dry enzymes and viruses. Radiation research. 1967 Apr 1; 30(4):855-71.
5. Dearnaley DP, Khoo VS, Norman AR, Meyer L, Nahum A, Tait D, et al. Comparison of radiation side-effects of conformal and conventional radiotherapy in prostate cancer: a randomised trial. The Lancet. 1999; 353(9149):267-72.
6. ICRU M. Report 36, International Commission on Radiation Units and Measurements, Bethesda, MD, 1983.
7. Cucinotta FA, Nikjoo H, Goodhead DT. Applications of amorphous track models in radiation biology. Radiation and environmental biophysics. 1999; 38(2):81-92.
8. Toossi MT, Ghorbani M, Sabet LS, Akbari F, Mehrpouyan M. A Monte Carlo study on dose enhancement and photon contamination production by various nanoparticles in electron mode of a medical linac. Nukleonika. 2015; 60(3):489-96.
9. Toossi MT, Ghorbani M, Akbari F, Sabet LS, Mehrpouyan M. Monte Carlo simulation of electron modes of a Siemens Primus linac (8, 12 and 14

- MeV). *Journal of Radiotherapy in Practice*. 2013; 12(4):352-9.
10. Toossi MT, Ghorbani M, Akbari F, Mehrpouyan M, Sabet LS. Evaluation of the effect of tooth and dental restoration material on electron dose distribution and production of photon contamination in electron beam radiotherapy. *Australasian physical & engineering sciences in medicine*. 2016; 39(1):113-22.
 11. Toossi MB, Khajetash B, Ghorbani M. Assessment of Neutron Contamination Originating from the Presence of Wedge and Block in Photon Beam Radiotherapy. *Journal of biomedical physics & engineering*. 2018; 8(1): 3.
 12. Toossi MT, Farhood B, Soleymanfard S. Evaluation of dose calculations accuracy of a commercial treatment planning system for the head and neck region in radiotherapy. *Reports of Practical Oncology & Radiotherapy*. 2017; 22(5):420-7.
 13. Kyllönen JE, Girard P, Uehara S, Wilson WE, Lindborg L, Nikjoo H. Energy deposition by monoenergetic ions in cylindrical targets Monograph. MRC RAGSU. 2003.
 14. Friedland W, Jacob P, Bernhardt P, Paretzke HG, Dingfelder M. Simulation of DNA damage after proton irradiation. *Radiation Research*. 2003; 159(3):401-10.
 15. Friedland W, Dingfelder M, Jacob P, Paretzke HG. Calculated DNA double-strand break and fragmentation yields after irradiation with He ions. *Radiation Physics and Chemistry*. 2005; 72(2-3):279-86.
 16. Friedland W, Dingfelder M, Kundrať P, Jacob P. Track structures, DNA targets and radiation effects in the biophysical Monte Carlo simulation code PARTRAC. *Mutation Research/Fundamental and Molecular Mechanisms of Mutagenesis*. 2011; 711(1-2):28-40.
 17. Chauvie S, Francis Z, Guatelli S, Incerti S, Mascialino B, Moretto P, et al. Geant4 physics processes for microdosimetry simulation: design foundation and implementation of the first set of models. *IEEE Transactions on Nuclear Science*. 2007; 54(6):2619-28.
 18. NIKJOO S, UEHARA WE, WILSON M, HOSHI DT, GOODHEAD H. Track structure in radiation biology: theory and applications. *International journal of radiation biology*. 1998; 73(4):355-64.
 19. Gilbert W. Towards a paradigm shift in biology. *Nature*. 1991; 349:99.
 20. Agostinelli S. GEANT4—a simulation toolkit. *Nuclear instruments and methods in physics research section A: Accelerators, Spectrometers, Detectors and Associated Equipment*. 2003; 506(3): 250-303.
 21. Allison J, Amako K, Apostolakis JE, Araujo HA, Dubois PA, Asai MA, et al. Geant4 developments and applications. *IEEE Transactions on nuclear science*. 2006; 53(1):270-8.
 22. Chauvie S, Francis Z, Guatelli S, Incerti S, Mascialino B, Montarou G, et al. Models of biological effects of radiation in the Geant4 Toolkit. In 2006 IEEE Nuclear Science Symposium Conference Record. 2006; 2: 803-5.
 23. Incerti S, Baldacchino G, Bernal M, et al. The Geant4-DNA project. *Int. J. Model. Simul. Sci. Comput*. 2010(1):157-178.
 24. Ebrahimi Loushab M. Assesment of Nuclear Interactions and Relative Biological Effectiveness in Carbon-Ion Therapy. 2015.
 25. Larsson S. Radiation transport calculations for narrow scanned photon beams using Geant4. 2002.
 26. Chauvie S, Scielzo G. Radiotherapy treatment planning with Monte Carlo on a distributed system. In 2003 IEEE Nuclear Science Symposium. Conference Record (IEEE Cat. No. 03CH37515). 2003; 3: 1765-9.
 27. Cirrone GA, Cuttone G, Guatelli S, Nigro SL, Mascialino B, Pia MG, et al. Implementation of a new Monte Carlo simulation tool for the development of a proton therapy beam line and verification of the related dose distributions. In 2003 IEEE Nuclear Science Symposium. Conference Record (IEEE Cat. No. 03CH37515). 2009; 3:1756-8.
 28. Loushab ME, Mowlavi AA, Hadizadeh MH, Izadi R, Jia SB. Impact of Various Beam Parameters on Lateral Scattering in Proton and Carbon-ion Therapy. *Journal of biomedical physics & engineering*. 2015; 5(4):169.
 29. Incerti S, Barberet P, Villeneuve R, Aguer P, Gontier E, Michelet-Habchi C, et al. Simulation of cellular irradiation with the CENBG microbeam line using Geant4. In 2003 IEEE Nuclear Science Symposium. Conference Record (IEEE Cat. No. 03CH37515). 2003; 3: 1759-64.
 30. Huang CY, Guatelli S, Oborn B, Allen BJ. Background dose for systemic targeted alpha therapy. 2011.
 31. Raisali G. Determination of Dose-Equivalent Response of A Typical Diamond Microdosimeter in Space Radiation Fields. *Iranian Journal of Medical Physics*. 2018; 15(1):39-47.
 32. Raisali G, Mirzakhani L, Masoudi SF, Semsarha F. Calculation of DNA strand breaks due to direct and indirect effects of Auger electrons from incorporated 123I and 125I radionuclides using the Geant4 computer code. *International journal of radiation biology*. 2013; 89(1):57-64.
 33. Strulab D, Santin G, Lazaro D, Breton V, Morel C. GATE (Geant4 Application for Tomographic Emission): a PET/SPECT general-purpose simulation platform. *Nuclear Physics B-Proceedings Supplements*. 2003; 125:75-9.
 34. Archambault L, Beaulieu L, Carrier JF, Castrovillari F, Chauvie S, Foppiano F, et al. Overview of Geant4 applications in medical physics. In 2003 IEEE Nuclear Science Symposium. Conference Record (IEEE Cat. No. 03CH37515). 2003; 3: 1743-5.
 35. Rodrigues P, Moura R, Ortigao C, Peralta L, Pia M, Trindade A, Varela J. Geant4 applications and developments for medical physics experiments. *IEEE Transactions on Nuclear Science*. 2004; 51(4):1412-19.
 36. Šefl M, Incerti S, Papamichael G, Emfietzoglou D. Calculation of cellular S-values using Geant4-DNA: the effect of cell geometry. *Applied Radiation and Isotopes*. 2015; 104:113-23.
 37. Cai Z, Pignol JP, Chan C, Reilly RM. Cellular dosimetry of 111In using Monte Carlo N-particle computer code: comparison with analytic methods and correlation with in vitro cytotoxicity. *Journal of Nuclear Medicine*. 2010; 51(3):462-70.

38. Tajik M, Rozatian AS, Semsarha F. Calculation of direct effects of ^{60}Co gamma rays on the different DNA structural levels: A simulation study using the Geant4-DNA toolkit. *Nuclear Instruments and Methods in Physics Research Section B: Beam Interactions with Materials and Atoms*. 2015; 346:53-60.
39. Pater P, Seuntjens J, El Naqa I, Bernal MA. On the consistency of Monte Carlo track structure DNA damage simulations. *Medical physics*. 2014; 41(12).
40. Villagrasa C, Francis Z, Incerti S. Physical models implemented in the GEANT4-DNA extension of the GEANT-4 toolkit for calculating initial radiation damage at the molecular level. *Radiation protection dosimetry*. 2010; 143(2-4):214-8.
41. Karamitros M, Mantero A, Incerti S, Friedland W, Baldacchino G, Barberet P, et al. Modeling radiation chemistry in the Geant4 toolkit. *Progress in nuclear science and technology*. 2011; 2(0): 503-8.
42. Mantero A. Modeling Radiation Chemistry and Biology in the Geant4 Toolkit. 2010.
43. Brenner DJ, Doll R, Goodhead DT, Hall EJ, Land CE, Little JB, et al. Cancer risks attributable to low doses of ionizing radiation: assessing what we really know. *Proceedings of the National Academy of Sciences*. 2003; 100(24):13761-6.
44. Hall EJ, Giaccia AJ. *Radiobiology for the Radiologist*. 2006.
45. Chauvie S, Francis Z, Guatelli S, Incerti S, Mascialino B, Montarou G, et al. Monte Carlo simulation of interactions of radiation with biological systems at the cellular and DNA levels: the Geant4-DNA project. In *Radiation Research*. 2006; 166: 676-7.
46. Huang CY, Oborn BM, Guatelli S, Allen BJ. Monte Carlo calculation of the maximum therapeutic gain of tumor antivasular alpha therapy. *Medical physics*. 2012; 39(3):1282-8.
47. Zaider M. Evidence of a neutron RBE of 70 (+/-50) for solid-tumor induction at Hiroshima and Nagasaki and its implications for assessing the effective neutron quality factor. *Health physics*. 1991; 61(5):631-6.
48. Freudenberg R, Wendisch M, Kotzerke J. Geant4-Simulations for cellular dosimetry in nuclear medicine. *Zeitschrift für Medizinische Physik*. 2011; 21(4):281-9.
49. Cai Z, Kwon YL, Reilly RM. Monte Carlo N-Particle (MCNP) modeling of the cellular dosimetry of ^{64}Cu : comparison with MIRDcell S values and implications for studies of its cytotoxic effects. *Journal of Nuclear Medicine*. 2017; 58(2):339-45.
50. Goddu SM. MIRD Cellular S values: Self-absorbed dose per unit cumulated activity for selected radionuclides and monoenergetic electron and alpha particle emitters incorporated into different cell compartments. *Society of Nuclear Medicine*; 1997.
51. Freudenberg R, Runge R, Maucksch U, Berger V, Kotzerke J. On the dose calculation at the cellular level and its implications for the RBE of $^{99\text{m}}\text{Tc}$ and ^{123}I . *Medical physics*. 2014; 41(6Part1).
52. Olive PL. The role of DNA single-and double-strand breaks in cell killing by ionizing radiation. *Radiation research*. 1998; 150(5s):S42-51.
53. Coghill MT. Radiobiological modeling using track structure analysis. 2012.
54. Barendsen GW, Walter HM. Effects of different ionizing radiations on human cells in tissue culture: IV. Modification of radiation damage. *Radiation research*. 1964; 21(2):314-29.
55. Dewey S. Lateral variations of radiobiological properties of therapeutic fields of ^1H , ^4He , ^{12}C and ^{16}O ions studied with Geant4 and microdosimetric kinetic model. *Physics in Medicine & Biology*. 2017; 62(14): 5884.
56. Chen Y, Li J, Li C, Qiu R, Wu Z. A modified microdosimetric kinetic model for relative biological effectiveness calculation. *Phys. Med. Biol.* 2018; 63(015008):14.
57. Burigo L, Pshenichnov I, Mishustin I, Bleicher M. Comparative study of dose distributions and cell survival fractions for ^1H , ^4He , ^{12}C and ^{16}O beams using Geant4 and Microdosimetric Kinetic model. *Physics in Medicine & Biology*. 2015; 60(8):3313.
58. Kase Y, Kanai T, Matsumoto Y, Furusawa Y, Okamoto H, Asaba T, et al. Microdosimetric measurements and estimation of human cell survival for heavy-ion beams. *Radiation research*. 2006; 166(4):629-38.
59. Burigo, L., et al., Comparative study of RBE and cell survival fractions for ^1H , ^4He , ^{12}C and ^{16}O beams using Geant4 and Microdosimetric Kinetic model. *arXiv preprint arXiv.2014;1403: 7929*.
60. Wyckoff H. International commission of radiation units and measurements. 1975..
61. Kase Y, Kanai T, Sakama M, Tameshige Y, Himukai T, Nose H, et al. Microdosimetric approach to NIRS-defined biological dose measurement for carbon-ion treatment beam. *Journal of radiation research*. 2011; 52(1):59-68.
62. Hosseini MA, Jia SB, Ebrahimi-Loushab M. Analysis of Relative Biological Effectiveness of Proton Beams and Iso-effective Dose Profiles Using Geant4. *Journal of biomedical physics & engineering*. 2017; 7(2): 95.
63. Guan F, Peeler C, Bronk L, Geng C, Taleei R, Randeniya S, et al. Analysis of the track-and dose-averaged LET and LET spectra in proton therapy using the geant4 Monte Carlo code. *Medical physics*. 2015; 42(11):6234-47.
64. Guan F, Bronk L, Titt U, Lin SH, Mirkovic D, Kerr MD, et al. Spatial mapping of the biologic effectiveness of scanned particle beams: towards biologically optimized particle therapy. *Scientific reports*. 2015; 5: 9850.
65. Huang CY, Guatelli S, Oborn BM, Allen BJ. Microdosimetry for targeted alpha therapy of cancer. *Computational and mathematical methods in medicine*. 2012; 2012. Seeram E, Davidson R, Bushong S, Swan H. Radiation dose optimization research: Exposure technique approaches in CR imaging: A literature review. *Radiography*. 2013; 19: 331-8.